



Biochromic silole derivatives: a single dye for differentiation, quantitation and imaging of live/dead cells

Journal:	<i>Materials Horizons</i>
Manuscript ID	MH-COM-07-2018-000799.R1
Article Type:	Communication
Date Submitted by the Author:	30-Jul-2018
Complete List of Authors:	<p>Chen, Sijie; The Hong Kong University of Science & Technology, Division of Biomedical Engineering Liu, Jianzhao; Zhejiang University, Department of Polymer Science and Engineering Zhang, Shouxiang; La Trobe University College of Science Health and Engineering, Department of Chemistry and Physics Zhao, Engui; Hong Kong University of Science and Technology, Department of Chemistry Yu, Chris Y. Y. ; Hong Kong University of Science and Technology, Chemistry Hushiaran, Roozbeh; La Trobe University College of Science Health and Engineering, Department of Chemistry and Physics Hong, Yuning; La Trobe University College of Science Health and Engineering, Department Tang, Ben Zhong; The Hong Kong University of Science and Technology, Department of Chemistry</p>

Title: Biochromic silole derivatives: a single dye for differentiation, quantitation and imaging of live/dead cells

Authors: Sijie Chen, Jianzhao Liu, Shouxiang Zhang, Engui Zhao, Yee Yung Yu, Roozbeh Hushiarian, Yuning Hong* and Ben Zhong Tang*

Contact: Y.Hong@latrobe.edu.au (YH) and tangbenz@ust.hk (BZT)

Conceptual Insight:

Measuring cell viability and determining the status of cell death are a routine but critical step in biological, medical and pharmaceutical research. This process is usually achieved by carefully selection of two different fluorescent probes with distinct emission spectrum and cellular uptake abilities. In this contribution, we develop two biochromic silole dyes and demonstrate a new approach for differentiating live and dead cells as well as quantitative analysis of cell viability by simply using one single probe. We anticipate that this concept based on the cell-permeable biochromic AIEgens will provoke other scientists to design new responsive materials to study important biological events.



Journal Name

ARTICLE

Biochromic silole derivatives: a single dye for differentiation, quantitation and imaging of live/dead cells

Sijie Chen,^{†ab} Jianzhao Liu,^{†ac} Shouxiang Zhang,^{†d} Engui Zhao,^a Yee Yung Yu,^a Roozbeh Hushiarian,^d Yuning Hong^{*ad} and Ben Zhong Tang^{*aef}

Received 00th January 20xx,
Accepted 00th January 20xx

DOI: 10.1039/x0xx00000x

www.rsc.org/

Differentiating between live and dead cells is a critical step for biological researchers, clinical doctors and pharmaceutical engineers when evaluating cell viability, for determining compound cytotoxicity and in the development of effective treatment for many diseases. Usually, careful selection and combination of two different dyes are required to differentiate and image both live and dead cells. In this work, we present a new method that can differentiate, quantify and image both live and dead cells at the same time through the use of a single, cell-permeable, biochromic fluorescent dye. Two silole-based hemicyanine dyes, Silo-Cy and Silo-2Cy are designed and synthesized. These dyes exhibit green fluorescence in both live and dead cells but much stronger green and red fluorescence from dead cells only. By collecting signals from the two distinct channels, we are able to image and discriminate between live and dead cells through fluorescence microscopy and quantify the cell viability via flow cytometry.

Introduction

Cell death, together with cell origin, development and proliferation, is an essential biological process for maintaining the normal functions of the human body.¹ Billions of cells die every single day in our bodies, regulating the homeostasis. Cells may suicide during fetal development, be terminated during aging, be sacrificed when injured or be killed when poisoned. Undesired cell death may cause inflammation or neurodegeneration, or even threaten people's lives.²⁻⁴ Alzheimer's disease, vascular diseases, rheumatoid arthritis, and psoriasis are just a few examples of possible consequences.⁵⁻⁸ On the other hand, without death, immortalized cells would also result in such other severe health problems as cancer.⁹ To cure and prevent these diseases,

scientists are continuously engaged in designing and screening different drugs as well as developing treatment methods to prevent undesired cell death, and promote the desired one.¹⁰⁻¹⁴ In their efforts, methods have been developed to possibly distinguish live and dead cells. However, it is still challenging to capture both scenes at the same time.¹⁵

According to the *Nomenclature Committee on Cell Death*, an organization comprising reputed researchers in the field of cell death worldwide, cells can be considered dead when they fulfil at least one of three criteria.¹⁶ The first criterion is that the plasma membrane has lost its integrity. Secondly, the cell has fragmented into apoptotic bodies and thirdly, the corpse or its fragments have been taken up by neighbouring cells. Additionally, as dying cells stop functioning, a decrease in metabolism can be observed at the cell population level.¹⁷ Supplementing this definition, there are currently a number of techniques available to assess cell death. They can be broadly grouped into either assays that measure *bona fide* cell death, or tests that quantify biochemical processes that are viewed as surrogate viability markers. Among preferred methods is the use of metabolic dyes which are fluorescent or colorimetric molecules, to assess the enzyme activity of cells, which indicates their viability.¹¹ (3-(4,5-Dimethylthiazol-2-yl)-2,5-diphenyl tetrazolium bromide (MTT) assay, based on the change of absorption to reveal the activity of reductase inside the cells, is one of the most widely used viability assays.^{18, 19} Unfortunately, the MTT assay process is tedious and laborious, and the results are not always reliable due to its susceptibility to factors such as over-confluency of the cells and the glucose concentration in the medium.²⁰ Another popular method for determining cell viability is to use fluorescent probes.²¹ Compared with MTT, fluorescent reporters have many advantages. They enjoy high

^a Department of Chemistry, Hong Kong Branch of Chinese National Engineering Research Center for Tissue Restoration and Reconstruction, Institute of Molecular Functional Materials, State Key Laboratory of Neuroscience, Division of Biomedical Engineering, and Division of Life Science., The Hong Kong University of Science and Technology, Kowloon, Hong Kong, China. Email: tanabenz@ust.hk

^b Ming Wai Lau Centre for Reparative Medicine, Karolinska Institutet, Hong Kong

^c MOE Key Laboratory of Macromolecular Synthesis and Functionalization, Department of Polymer Science and Engineering, Zhejiang University, Zheda Road 38, Hangzhou 310027, China

^d Department of Chemistry and Physics, La Trobe Institute for Molecular Science, La Trobe University, Melbourne, Victoria 3086 Australia. Email: Y.Hong@latrobe.edu.au

^e HKUST-Shenzhen Research Institute, Hi-tech Park, Nanshan, Shenzhen 518057.

^f China NSFC Center for Luminescence from Molecular Aggregates, SCUT-HKUST Joint Research Institute, State Key Laboratory of Luminescent Materials and Devices, South China University of Technology, Guangzhou 510640, China

[†] These authors contribute equally.

Electronic Supplementary Information (ESI) available: Emission spectra at different pH, cytotoxicity, confocal imaging and flow cytometry data. See DOI: 10.1039/x0xx00000x

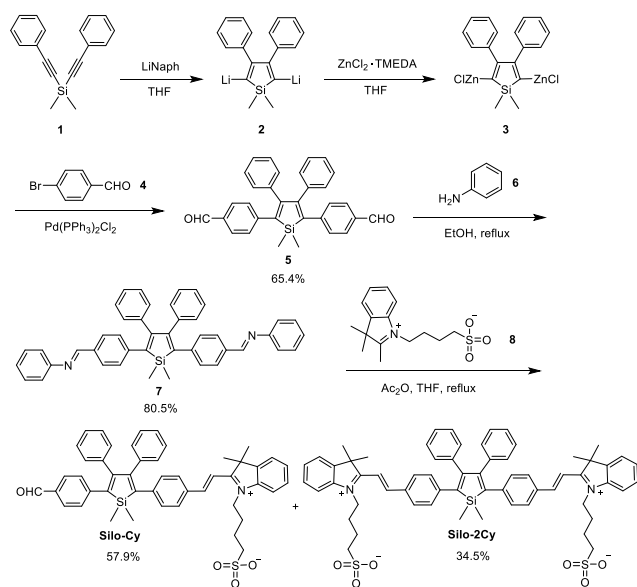


Fig. 1 Synthetic route to Silo-Cy and Silo-2Cy.

signal to noise ratio, excellent sensitivity and capacity of visual observation. Usually two dyes are needed: one dye to stain the live cells and the other to stain the dead cells.²² Fluorophores caged with acetomethoxy moieties can turn on their fluorescence by the activation of intracellular esterase, and hence respond to live cells only.²³ For dead cell staining, cell-impermeable dyes are chosen as these can only enter the compromised cell membrane of dead cells.²⁴ Cell viability is thus obtained by using a combination of these two types of dyes. It should be noted though, that careful selection of the combination is necessary so that no spectral overlapping of the dyes occurs.²⁵

Aggregation-induced emission (AIE) molecules have been shown to have great potential as biosensors and probes.^{26–30} We have previously reported a pH sensitive AIE dye, tetraphenylethene-cyanine adduct (TPE-Cy).^{31, 32} TPE-Cy undergoes red to blue emission transition in alkaline conditions with pH >10. Interestingly, in the presence of lipids, the dye shifts its colour transition point to the physiological range to exhibit blue emission in a neutral buffer solution. This biochromic effect prompted us to further improve the system for multifunctional imaging. In this work, we have built on the previous results to design and synthesize two silole derivatives with cyanine moieties, Silo-Cy and Silo-2Cy. Similar to TPE, silole is an archetype of the AIE luminogens: it is non-emissive when molecularly dissolved but becomes highly luminescent in the aggregate state or when intramolecular motions are restricted.³³ With extended π -conjugation systems, these two dyes emit strong red and near infrared colours in the aggregate state.^{34–37} They are also pH sensitive and shift the emission colour from red to green at high pH. Both of them are cell-permeable, staining most of the cytoplasmic region with green fluorescence and the acidic compartments with weak red fluorescence. Intriguingly, their fluorescence intensity differs by orders of magnitude in live and dead cells, along with distinct

intracellular distribution pattern, allowing the use of only one dye to achieve the differentiation and quantitation of both live and dead cells through fluorescence microscopy and flow cytometry.

Results and discussion

Dye synthesis and photophysical characterisation

We prepared Silo-Cy and Silo-2Cy by the synthetic route shown in Fig. 1 and obtained a reasonable yield. The reaction intermediates and final products were well characterized by ¹H and ¹³C NMR and high-resolution mass spectrometry (HRMS).

Both Silo-Cy and Silo-2Cy are sensitive to pH changes. With the increase of pH from 1 to 9, the absorption of Silo-Cy at 450 nm remained almost unchanged (Fig. S1A). When the pH value was above 10, the absorption dropped dramatically and the peak at 450 nm disappeared when the pH reached 13 (Fig. S1B). Similarly, Silo-2Cy showed an absorption peak at 470 nm in acidic aqueous buffer (Fig. S1C). Alkalinization at a pH of 9 to 13 led to the vanishing of this absorption peak with a shoulder peak remaining at about 400 nm (Fig. S1D). These results indicated that the hydroxyl ions at high pH act as nucleophiles, which would break down the conjugation between hemicyanine and the silole moieties and result in the disappearance of the absorption at the longer wavelength.^{31, 32}

The response to pH was also reflected in the emission spectra. When excited at 470 nm, Silo-Cy and Silo-2Cy emitted at the red region with an emission maximum at 640 nm and 670 nm at neutral pH, respectively (Fig. S2). With the decrease of pH, the red emission was intensified (Fig. S2B, D), implying that both dyes are less soluble and thus aggregate at low pH. Under alkaline conditions, the red emission was suppressed and a new shoulder peak emerged in the green region. The ratio of the two emission peaks showed a linear relationship with the pH value in the range of pH 3 to 8, implying its potential use for pH sensing in the physiological region.

Previously we have found that TPE-Cy can shift its transition point of the red-to-blue emission from extracellular pH 10 to intracellular physiological pH range, possibly due to the involvement of intracellular lipid components. To verify whether Silo-Cy and Silo-2Cy would exhibit the same behaviour, we examined the emission change of the dye molecules at the physiological pH range in the presence and absence of phospholipid. 1,2-Dioleoyl-glycero-3-

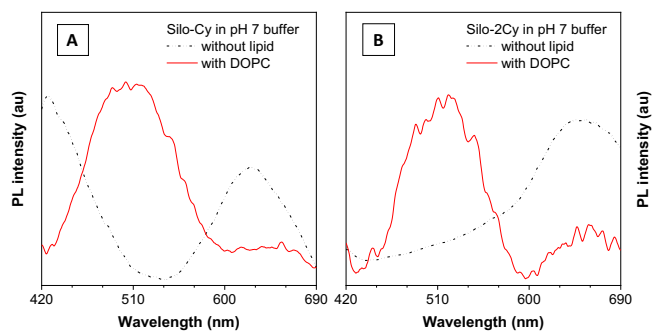


Fig. 2 Emission spectra of (A) Silo-Cy and (B) Silo-2Cy in buffer solution in the presence and absence of DOPC. PL intensity is normalized. [Silo-Cy] = 5×10^{-6} M; [DOPC] = 1 mg/mL; λ_{ex} : 370 nm.

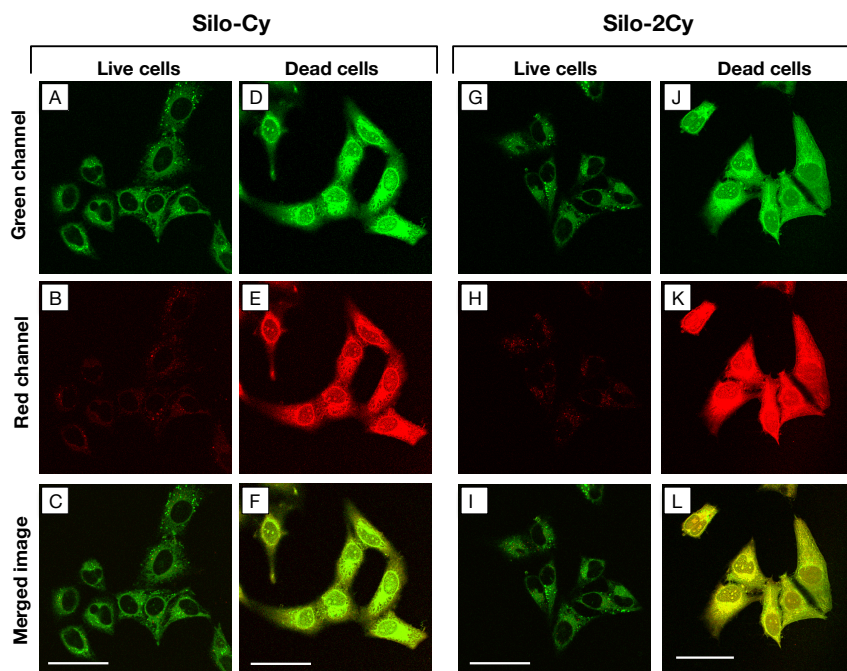


Fig. 3 Comparison of confocal images of (A, B and C) live and (D, E and F) dead HeLa cells incubated with Silo-Cy for 2 h and (G, H and I) live and (J, K and L) dead HeLa cells incubated with Silo-2Cy for 2 h. The green channel was under excitation of 405 nm and red channel 488 nm. Images from two channels were then merged [dye] = 4×10^{-6} M. Scale bars: 50 μ m.

phosphocholine (DOPC) was chosen as a model lipid of cell membrane. When excited at 370 nm, which corresponds to the green form of the dyes, both Silo-Cy and Silo-2Cy emitted predominantly in the red region with emission maximum at approx. 630 nm (Fig. 2). The peak at around 420 nm was most likely from the Raman scattering owing to the aggregate formation of hydrophobic Silo-Cy in aqueous media (Fig. 2A). In the presence of DOPC, we observed that the fluorescence intensity at around 630 nm attenuated, while another peak at \sim 510 nm emerged at the same pH condition. This result suggested that both dyes are potentially biochromic: they tend to change their emission colours in the presence of biological molecules, e.g. lipid.

Imaging live/dead cells by a single dye

The biochromic property of Silo-Cy and Silo-2Cy prompted us to examine their behaviours in cells. Prior to applying the dyes for cell staining, we evaluated the cytotoxicity of the compounds using MTT assay. The results showed that the viability of the HeLa cells was not obviously affected upon incubation with up to 5 μ M of Silo-Cy and Silo-2Cy for 24 hours (Fig. S3).

After verification of the biocompatibility of Silo-Cy and Silo-2Cy, we employed the dyes for live cell imaging. These dyes are cell permeable. When excited at 488 nm, weak, punctate patterns of the red fluorescent signals were observed in the cytoplasmic region. When excited at 405 nm, the obtained green fluorescent signals distributed mainly in the membrane bounded organelles, including tubular mitochondria, which is different from the signals from the red emission window (Fig. S4). Since Silo-Cy and Silo-2Cy shifted their emission peak to the green region in the neutral or alkalinized pH in the lipid-containing environment, once they entered the cells, the

red-to-green colour transition occurred. This suggests a reason for the majority of the stained region emitting a green light in live cells.

During the imaging of live HeLa cells, we noticed a few cells glowing intensely with red emission in the observation window. We speculated that this group may be cells which were dying during the culture process. To verify our hypothesis, dead HeLa cells killed by 70% ethanol fixation were stained with Silo-Cy and Silo-2Cy, followed by the same protocol used for staining live cells. By comparing the signals from the green and red channels, the live cells were stained in the cytoplasmic region only (Fig. 3A, G). The nucleus was excluded, revealing a clear boundary of the nuclear envelope. Weak emission observed in the red channel was most likely from the acidic compartments like lysosomes (Fig. 3B, H). Conversely, for dead cells, the entire cell including the nucleus was stained with strong signals from both green (Fig. 3D, J) and red channels (Fig. 3E, K). These dyes are cell permeable but the strict selectivity of the nuclear membrane restricts the free diffusion of the dye molecules into the nucleus.³⁸ For dead cells, the selectivity of the nucleus membrane was compromised, exposing the nucleus to be stained.

Differentiation of cell necrosis and apoptosis by imaging

Hydrogen peroxide (H_2O_2) is a major and the most important source of cellular reactive oxygen species (ROS).³⁹ Many studies have reported that low concentration of H_2O_2 leads to cell apoptosis while high concentration treatment changes the death mode to necrosis.⁴⁰ In order to investigate the performance of the two dyes in discrimination of apoptosis and necrosis, we induced cell death with 0.2 mM and 2 mM of H_2O_2 for 6 hours respectively.

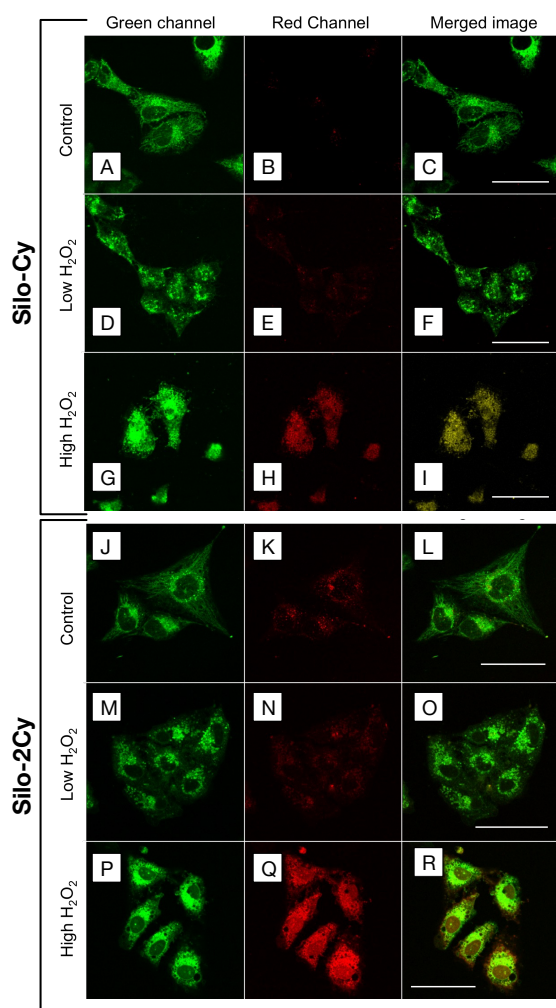


Fig. 4 Comparison of confocal images of HeLa cells incubated with [Silo-Cy] = 4×10^{-6} M (A–I) and [Silo-2Cy] = 4×10^{-6} M (J–R). For low and high H₂O₂ treatment respectively, 0.2 mM and 2 mM of H₂O₂ for 6 hours was used. Subsequently, the cells were incubated with either Silo-Cy or Silo-2Cy for 2 hours and imaged with excitation of 405 nm for the green channel and 488 nm for the red channel. Scale bar: 50 μ m.

As is shown in Fig. 4, upon staining the cells after H₂O₂ treatment, fluorescence from both green and red channels was dramatically enhanced for necrotic cells compared with the control group. The apoptotic cells, however, did not show a significant increase in fluorescence in spite of the change in cell morphology (Fig. 4D–F and 4M–O). Cell death through a high level of H₂O₂ induced necrosis led to high red and green signals after staining with Silo-2Cy, which is consistent with those of the stained fixed cells (Fig. 4G–I and 4P–R). Distinct vacuolization in the cytoplasmic region could be visualized. On the other hand, for cells that underwent apoptosis, the morphology changes of certain organelles could be captured. In particular, the tubular networks of mitochondria (control cells) were interrupted and fragmented into punctiform (low H₂O₂) which is one of the features of apoptotic cells.⁴¹

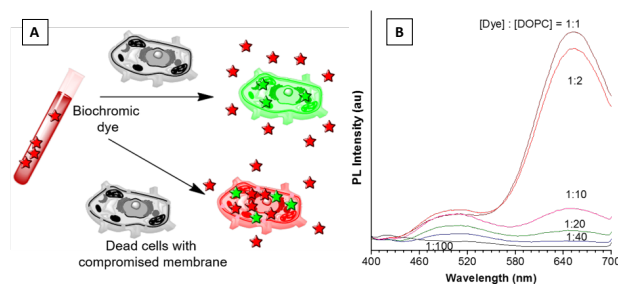


Fig. 5 (A) The proposed working mechanism of using a biochromic dye (e.g. Silo-Cy or Silo-2Cy) for live/dead cell staining. (B) PL spectra of different amount of Silo-Cy in the presence 0.1 mM DOPC. λ_{ex} : 370 nm.

The different staining patterns of apoptotic and necrotic cells can be attributed to the change of membrane integrity. Necrotic cells resulting from acute insults lose membrane integrity,⁴² which allows large quantities of dye molecules to flood in, and thus resulting in a strong fluorescence from all intracellular compartments. However, apoptosis is a programmed cell death, during which the membrane integrity is always preserved for the purpose of inhibiting the inflammation response of the living body.⁴³ With only a limited number of dye molecules in the cell, the fluorescence from apoptotic cells was much lower than that from necrotic cells. Since both Silo-Cy and Silo-2Cy are lipophilic and cell permeable, they were able to light up the membrane-bound organelles in cells, facilitating the monitoring of the morphological changes of these intracellular membranes and organelles during the biological events.

In addition to the difference in intracellular distribution between live and dead cells, the intensity was also dramatically changed. We suspect that the distinct membrane integration of the live/dead cells

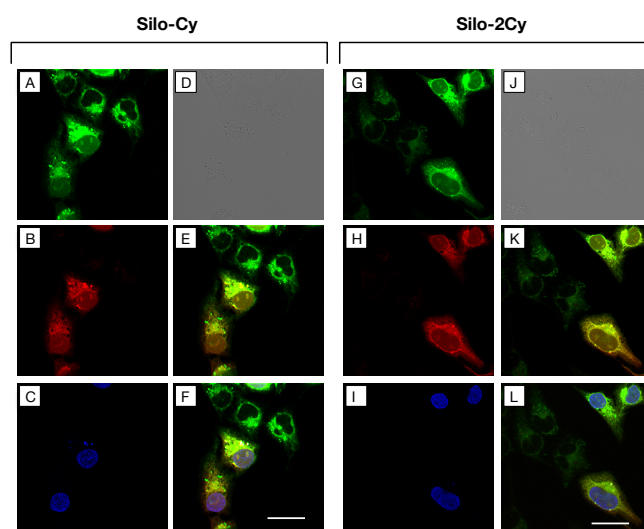


Fig. 6 Live and dead cells mixture co-stained with Silo-Cy/Silo-2Cy and TO-PRO-3. A and G are the green channel. B and H are the red channel. C and I are nuclei of dead cells stained by TO-PRO-3. D and J are bright field images. E and K are merged images from the red and green channels. F and L are merged images from TO-PRO-3 and the red and green channels of the cells stained with Silo-Cy and Silo-2Cy respectively. Scale bar: 30 μ m.

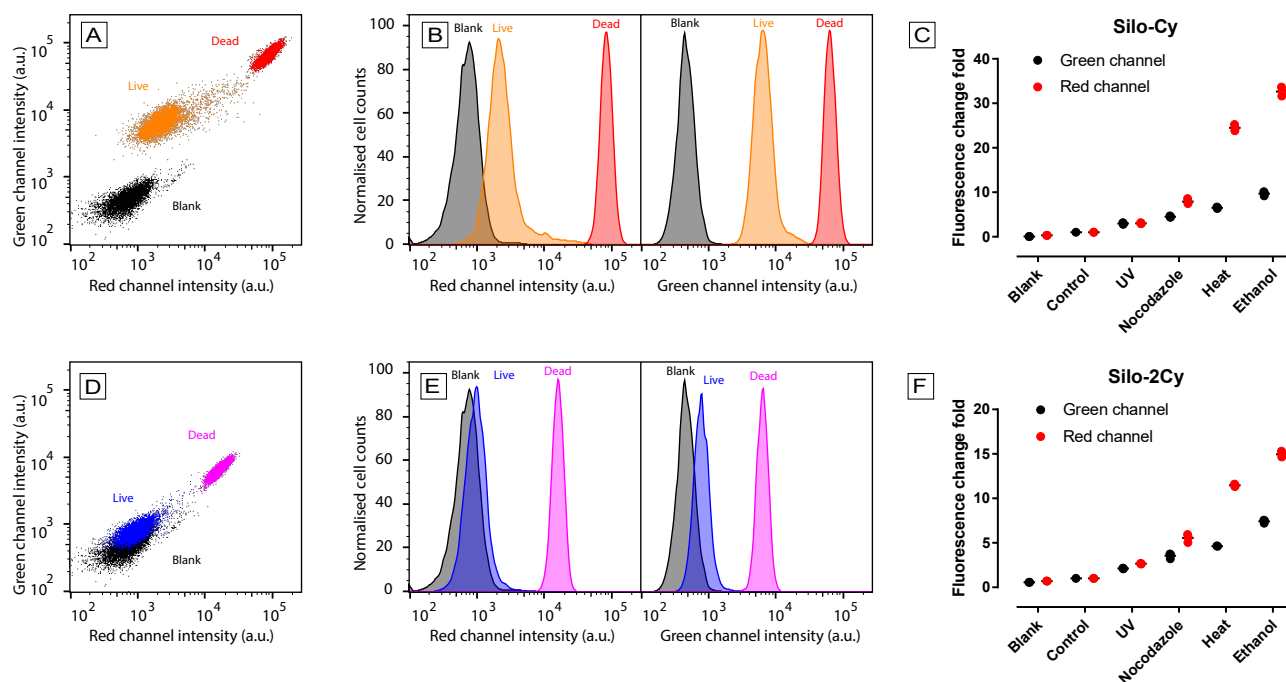


Fig. 7 Quantitative analysis of live and dead cells by flow cytometry. (A,B,D,E) Scatter plots and histogram of live or dead HeLa cells stained with (A,B) Silo-Cy and (D,E) Silo-2Cy by flow cytometry. Green channel: $\lambda_{\text{ex}} = 405 \text{ nm}$; $\lambda_{\text{em}} = 510 \pm 50 \text{ nm}$ and red channel: $\lambda_{\text{ex}} = 488 \text{ nm}$; $\lambda_{\text{em}} = 670 \pm 14 \text{ nm}$. Unstained live cells are shown as a blank (black). Stained live cells, set as the control, and stained dead cells, killed by 70% ethanol treatment for 10 minutes, are shown as dots with different colours. 6000 cells are shown for each cell population in the scatter plots. For histogram, cell counts are normalised to the same height to clearly compare the fluorescence intensity distribution of each cell population in red or green channel. (C,F) Fold of fluorescence increase of HeLa cells under different stress conditions stained by (C) Silo-Cy or (F) Silo-2Cy, $n = 3$ biological replicates; mean \pm s.e.m. Fluorescence change fold is calculated by the ratio of median stress fluorescence to average of median negative control fluorescence.

may play a role here (Fig. 5A). The membrane of the live cells possibly serves as a barrier, limiting the number of dye molecules that enter the cell. With a relatively small number of dye molecules, the total lipids in the cell were adequate to convert them into green form, giving green fluorescence in the membrane-bound organelles and weak red fluorescence in the acidic lysosome region. On the other hand, the dead cells with compromised cell membrane allowed excess dye molecules to flow into the cell, distributing all over the cell including the nuclear region. With the increase of dye quantity, green signals were enhanced. Meanwhile, due to the excess amount of dyes, the lipid to dye ratio became uneven. As a result, a quantity of dye molecules did not interact with the lipids and emitted the original red colour identical to the extracellular scenario. Therefore, by collecting signals from these two distinct channels, we were able to differentiate live and dead cells easily.

To validate our hypothesis, we added different amounts of Silo-Cy (Fig. 5B) or Silo-2Cy (Fig. S5) into the same amount of lipid in a neutral pH buffer. Originally, in the presence of an excess amount of DOPC (e.g. dye/lipid 1:40), the green emission was stronger than the red emission. As more dye molecules were added, the red fluorescence emerged and became comparable to the green emission. Further increasing the ratio led to a stronger red emission and a diminished

green emission. When the dye/lipid ratio reached 1:2 or 1:1, the red signals were amplified to a much higher level. These results were concordant with our explanation of the dye's ability to differentiate live and dead cells.

To further illustrate capability in live/dead cell discrimination, we mixed a fraction of dead cells with live cells before incubation with the dyes, so that both dead and live cells could be imaged in the same imaging field under identical conditions. In our experiment, the cells were co-stained with TO-PRO-3 (Fig. 6C, I), which selectively light up the nuclei of dead cells.⁴⁴ Note that TO-PRO-3 signal does not bleed-through to either the green or the red channel of Si-Cy and Silo-2Cy (Fig. S6). As shown in Fig. 6, all the stained cells exhibited green fluorescence, whereas only dead cells emitting an intense red colour could be visualized in the red channel. From the overlay image, live/dead cells can be clearly differentiated: the live cells showed green emission and the dead cells were yellow by virtue of similar intensity of both strong green and red fluorescence. Silo-2Cy exhibited a similar property as depicted below. Using this method, staining and differentiation of live/dead cells was successfully achieved with a single dye.

High-throughput quantitation of cell viability

The results of live/dead cell imaging obtained from a confocal microscope encouraged us to continue to investigate their application for high-throughput and quantitative analysis. Flow cytometry is a commonly used tool for this purpose. Its light source is laser-based and it is suitable for simultaneous detection of multichannel fluorescent signals.⁴⁵ We thus performed flow cytometry assay to obtain fluorescence changes in both green and red channels of cells under different stimulant treatments (Fig. 7). Live HeLa cells without staining as a blank was shown as black dots exhibiting very low signals from both green and red channels in the scatter plots (Fig. 7A, D). Live cells and dead cells killed by 70% ethanol were shown for comparison. The live cells stained by Silo-Cy exhibited significantly increased signal in the green channel and medium increased signal in the red channel (Fig. 7B). The stained dead cells displayed a fluorescence change of more than one order of magnitude in both green and red channels, when compared to the negative control. Silo-2Cy behaved similarly but with much lower background signals in live cells under the same acquisition conditions (Fig. 7D, E). These results were consistent with our observation under confocal microscope (Fig. 3).

In the abovementioned scenario, the dead cell populations can be well separated from the live cells with Silo-Cy or Silo-2Cy staining by flow cytometry. We thus applied the two dyes on assessing the viability of cells treated with other chemical, physical, and biological stressors, and compared the fold of fluorescence change in each channel individually of cells stained either by Silo-Cy or Silo-2Cy under stress treatment, normalised to the negative control signals (Table S1). We assumed that the signals from stained live cells remained the same across different experiments (Table S2).

We tested the dyes in the following conditions which induce the apoptotic process and eventually cell death. UV irradiation would trigger a complicated cellular response termed as the UV response, which involves the post-translational activation of pre-existing transcriptional factors, such as NF- κ B and AP-1, and proinflammatory gene products.⁴⁶ Prolonged UV exposure eventually causes apoptosis by inhibition of DNA synthesis and cell death pathway. The cells were exposed to UV light (200 J/m²) and then cultured in dark for another 24 hours before the dye staining. Heat stress increases ROS generation and activates the apoptotic process through mitochondrial signalling pathway.⁴⁷ We exposed another batch of cells to 55 °C for 2 hours and followed by normal culture condition (37 °C) for 12 hours prior to dye staining. Nocodazole is an antineoplastic agent that arrests the cell cycle through synchronization.⁴⁸ It reduces the microtubule dynamic turnover and inhibits mitotic spindle functions. Eventually it activates the JNK/SAPK signalling pathway and induces apoptosis.⁴⁹

As shown in Fig. 7C and 7F, both red and green fluorescence increased concomitantly with each other when cells experienced stress conditions. More specific, the red fluorescence change reached up to 33 and 15 folds for Silo-Cy and Silo-2Cy, respectively, and a nearly 10 folds maximal increase in the green channel of both dyes. The patterns of fluorescence change fold upon other stressors for both dyes were similar to those of ethanol treatment but to a smaller extent. UV-induced cell apoptosis caused about 3 and 2 folds

fluorescence increase in the red channels for Silo-Cy and Silo-2Cy, respectively. Upon nocodazole treatment, which arrests the cells in prometaphase, about 8- and 5-fold increase could be observed in the red channel of the dyes. More severe treatment, such as hypothermic conditions at 55 °C led to about 25- and 11-fold increase of the red fluorescence signals.

Interestingly, the green fluorescence increased more linearly with the strength of the stress, whereas the red fluorescence exhibited small increase with weak stressors but a drastic enhancement when cells were overstressed. In the early apoptosis event such as under UV radiation or nocodazole treatment, the cell membrane was only partially compromised and therefore only a small number of dye molecules entered the cells and exhibited green fluorescence. At this stage, red-to-green emission shift was predominant, giving more fluorescence increase in the green channel rather than the red channel. During the late apoptosis, such as after high-temperature treatment, the cell membrane is more compromised and excessive dyes can get into the cells, resulting in strong red fluorescence. These results demonstrated the feasibility of using Silo-Cy or Silo-2Cy as tools for detecting not only the cell viability but also differentiating the early and late apoptotic states.

Conclusions

This work has put forward a novel, simple and convenient method for live/dead cell imaging, discrimination and quantitation, using a single cell permeable biochromic dye. In the experiments described, we designed and synthesized two red emitting silole based hemicyanine dyes, Silo-Cy and Silo-2Cy. These two dyes possess biochromic characteristic: in the presence of biomolecules such as phospholipid, the emission colour would change from red to green. Silo-Cy and Silo-2Cy are cell-permeable with negligible cytotoxicity. When entering cells, the dyes were observed to stain most membrane-bound organelles with green fluorescence and acidic lysosomes with red emission. The dead cells with compromised membranes allowed large numbers of dye molecules to irrupt, the dyes spreading over the entire cytoplasmic region, including the nuclear region, and displaying strong emission from both green and red channels. The significant difference in imaging patterns and intensity between the two dyes on the live and dead cells offers a new approach to differentiating live and dead cells. By using flow cytometry with just one dye, we were able to simultaneously and easily quantify not only cell viability but also identifying cells in the early and late apoptosis.

Experimental section

Materials and instruments

Hexane and tetrahydrofuran (THF) were distilled from sodium benzophenone ketyl immediately prior to use. Dichloromethane (DCM) was distilled over calcium hydride. Dichlorobis(triphenylphosphine)palladium(II), ZnCl₂·TMEDA, aniline, 4-bromobenzaldehyde, 2,3,3-trimethylindolenine, 1,4-butanediol, Ac₂O, and other chemicals were all purchased from Aldrich and used as received without further purification.

Compound **8** was synthesized according to the published literature.⁵⁰

Minimum essential medium (MEM), Dulbecco's Modified Eagle Medium (DMEM), fetal bovine serum (FBS), penicillin and streptomycin, 3-(4,5-dimethyl-2-thiazolyl)-2,5-diphenyltetrazolium bromide (MTT), sodium dodecyl sulfate (SDS), TO-PRO-3 were purchased from Life technologies. 4-(2-hydroxyethyl)-1-piperazineethanesulfonic acid (HEPES) was purchased from Acros. 1,2-Dioleoyl-glycero-3-phosphocholine (DOPC) was purchased from Avanti Polar Lipids, Inc. All other reagents used in this study were purchased from Sigma-Aldrich. Nocodazole was gift from the laboratory of Patrick Humbert (La Trobe University). pH buffer was prepared using citric acid and Na₂HPO₄,⁵¹ with the pH value confirmed with a pH meter (Beckman Φ 340 pH/Temp meter).

For PL measurements and cell staining, unless otherwise specified, the aqueous solutions of siloles were prepared by adding an aliquot of stock solution of 1 mM dye in DMSO into the aqueous buffers. For reaction with DOPC, the incubation was at room temperature for overnight to reach the equilibrium of the reaction.

¹H and ¹³C NMR spectra were measured on a Bruker ARX 400 NMR spectrometer using chloroform-*d* or methanol-*d*₄ as solvent and tetramethylsilane (TMS) as an internal reference. UV absorption spectra were taken on a Milton Ray Spectronic 3000 array spectrophotometer. PL spectra were recorded on a Perkin-Elmer LS 55 spectrofluorometer. High-resolution mass spectra (HRMS) were measured on a GCT Premier CAB 048 mass spectrometer operating in MALDI-TOF model. For confocal imaging, the data was acquired with a Zeiss laser scanning confocal microscope (model: LSM7 DUO). Flow cytometry analyses were performed using FACS Canto II flow cytometry (Becton Dickinson).

Dye synthesis and characterization

Preparation of 1. To a THF solution of phenylacetylene (4.0 mL, 36.4 mmol) was added *n*-BuLi (25.0 mL, 40.1 mmol, 1.6 M solution in hexane) at -78 °C. After stirring at -78 °C for 4 h, dichlorodimethylsilane (2.2 mL, 18.2 mmol) was added. The mixture was warmed to room temperature and stirred overnight. The solvent was removed under reduced pressure. The mixture was dissolved in DCM and washed with brine and water. The organic layer was dried over magnesium sulfate. The crude product was purified by a silica-gel column using hexane as eluent. A colourless solid was obtained in 86.1% yield. ¹H NMR (400 MHz, CDCl₃), δ (ppm): 7.57 (m, 4H), 7.36 (m, 6H), 0.55 (s, 6H). ¹³C NMR (100 MHz, CDCl₃), δ (ppm): 132.1, 128.9, 128.2, 122.6, 105.9, 90.6, 0.45. HRMS (MALDI-TOF), *m/z* 260.1013 (M⁺, calcd 260.1021).

Preparation of 5. A mixture of lithium (0.056 g, 8 mmol) and naphthalene (1.04 g, 8 mmol) in 8 mL of THF was stirred at room temperature under nitrogen for 3 h to form a deep dark green solution of LiNaph. The viscous solution was then added dropwise to a solution of **1** (0.52 g, 2 mmol) in 5 mL of THF over 4 min at room temperature. After stirring for 1 h, the mixture was cooled to 0 °C and then diluted with 25 mL THF. A black suspension was formed upon addition of ZnCl₂-TMEDA (2 g, 8

mmol). After stirring for an additional hour at room temperature, a solution of 4-bromobenzaldehyde (0.78 g, 4.2 mmol) and PdCl₂(PPh₃)₂ (0.08 g, 0.1 mmol) in 25 mL of THF was added. The mixture was refluxed overnight. After being cooled to room temperature, 100 mL of H₂O was added and the mixture was extracted with DCM. The combined organic layer was then washed with brine and water and then dried over magnesium sulfate. Following solvent evaporation under reduced pressure, the residue was purified by a silica-gel column using gradient DCM/hexane (50:50 to 100:0 v/v) as eluent. The product was obtained as a yellow solid in 65.4% yield (0.62 g, 1.3 mmol). ¹H NMR (400 MHz, CDCl₃), δ (TMS, ppm): 9.89 (s, 2H), 7.65 (d, 4H), 7.10–6.98 (m, 10H), 6.78 (d, 4H), 0.51 (s, 6H). ¹³C NMR (100 MHz, CDCl₃), δ (TMS, ppm): 191.7, 155.8, 146.6, 142.2, 137.6, 133.7, 129.7, 129.6, 129.1, 127.6, 126.9, -4.1. HRMS (MALDI-TOF): *m/z* 470.1750 (M⁺, calcd 470.1702).

Preparation of 7. Compound **5** (0.23 g, 0.48 mmol) was dissolved and refluxed in 25 mL of anhydrous ethanol under nitrogen. After **5** was completely dissolved, 0.53 mL (5.8 mmol) of aniline was added and further refluxed overnight. After cooled by ice water, precipitates were formed and filtered out. The residue was washed twice by cold ethanol and vacuum-dried without further purification. The product was obtained as a yellow solid in 80.5% yield (0.24 g, 0.39 mmol). ¹H NMR (400 MHz, CDCl₃), δ (TMS, ppm): 8.36 (s, 2H), 7.67 (d, 4H), 7.37 (t, 4H), 7.21 (t, 2H), 7.17 (d, 4H), 7.08 and 6.99 (m, 10H), 6.83 (d, 4H), 0.51 (s, 6H). ¹³C NMR (100 MHz, CDCl₃), δ (TMS, ppm): 160.1, 155.1, 152.2, 143.4, 142.0, 138.3, 133.6, 129.9, 129.2, 129.1, 128.6, 127.6, 126.6, 125.8, 120.8, -3.9. HRMS (MALDI-TOF): *m/z* 621.2725 ([M + H]⁺, calcd 621.2726).

Preparation of Silo-Cy and Silo-2Cy. Compounds **7** (0.16 g, 0.25 mmol) and **8** (0.18g, 0.6 mmol) were vacuum-dried and refilled with nitrogen three times. Afterwards, 25 mL of freshly distilled THF and 5 mL of Ac₂O were injected into the mixture and refluxed overnight. After cooling to room temperature, the solvents were evaporated under reduced pressure and the residues extracted with chloroform and water. The organic layer was further washed with brine and water and dried over magnesium sulfate. After the solvent evaporation, the crude product was purified by a silica-gel column using gradient chloroform/methanol (v/v from 90:10 to 0:100) mixture as eluent. Red solids Silo-Cy and Silo-2Cy were obtained in 57.9% and 34.5% yields, respectively.

Characterization data of Silo-Cy. ¹H NMR (400 MHz, CDCl₃), δ (TMS, ppm): 9.89 (s, 1H), 8.04 (dd, 2H), 7.92 (d, 2H), 7.72 (s, 1H), 7.65 (d, 2H), 7.62-7.48 (m, 4H), 7.11 (d, 2H), 7.08-6.98 (m, 8H), 7.79 (t, 4H), 4.88 (t, 2H), 3.08 (t, 2H), 2.25-2.10 (m, 4H), 1.76 (s, 6H), 0.51 (s, 6H). ¹³C NMR (100 MHz, CDCl₃), δ (TMS, ppm): 191.8, 181.1, 156.2, 155.8, 155.4, 147.1, 146.6, 143.0, 142.8, 142.6, 140.6, 137.7, 137.6, 133.7, 131.5, 131.4, 130.0, 129.9, 129.8, 129.7, 129.6, 129.5, 129.1, 127.7, 127.6, 126.9, 126.8, 122.4, 115.0, 111.8, 52.0, 49.6, 47.4, 27.1, 26.9, 22.4, -4.1. HRMS (MALDI-TOF): *m/z* 748.2709 ([M + H]⁺, calcd 748.2917); 770.2534 ([M + Na]⁺, 770.2736).

Characterization data of Silo-2Cy. ¹H NMR (400 MHz, CD₃OD), δ (TMS, ppm): 8.38 + 8.35 (s + d, 2H), 7.90 (d, 4H), 7.87 (m, 2H),

7.75 (m, 2H), 7.68–7.58 (m, 6H), 7.16 (d, 4H), 7.10–7.00 (m, 6H), 6.85 (dd, 4H), 4.68 (t, 4H), 2.91 (t, 4H), 2.15 (p, 4H), 1.98 (p, 4H), 1.83 (s, 12H), 0.55 (s, 6H). ¹³C NMR (100 MHz, CD₃OD), δ (TMS, ppm): 183.6, 158.0, 156.2, 147.5, 145.2, 144.0, 142.2, 139.5, 133.5, 131.8, 131.0, 130.9, 130.6, 128.9, 128.1, 124.1, 116.2, 112.5, 53.9, 51.2, 47.8, 28.2, 26.7, 23.3, -4.0. HRMS (MALDI-TOF): m/z 1026.4275 ([M+2H]⁺, calcd 1026.4132); 1048.4103 ([M+H+Na]⁺, 1048.3951).

Cell culture

HeLa cells were cultured in MEM or DMEM in a humidity incubator at 37 °C with 5% CO₂. The medium contained 10% FBS, 100 units/mL penicillin and 100 μ g/mL streptomycin.

Cell viability test

Cells were seeded in 96-well plates at density of 5000 cells/well. After overnight culture, the medium in each well was replaced by a fresh phenol-red-free-medium containing different concentrations of Silo-Cy or Silo-2Cy. DMSO contents in the medium had the final concentration of 0.5%. After 24 hours treatment, 10 μ L MTT solution (5 mg/mL in phosphate buffer solution) was added into each well. After 4 hours incubation at 37 °C, 100 μ L SDS-HCl solution (10% SDS and 0.01 M HCl) was added to each well and the absorbance of each well at 570 nm was recorded by the plate reader (Perkin-Elmer Victor3™).

Cell staining and imaging

HeLa cells were seeded in a 35 mm glass-bottom tissue culture plate. After overnight culture, the cells were stained with dye for 2 h in a humidity incubator at 37 °C with 5% CO₂. Before imaging, the cells were washed with a phosphate buffered saline (PBS) (pH 7.4) solution three times. The cells were then placed in a phenol red-free MEM medium containing 10 mM HEPES (pH 7.4) for confocal imaging. Confocal imaging was performed with a Zeiss LSM710 laser scanning confocal microscope and a 63 \times objective: for green channel, λ_{ex} : 405 nm, λ_{em} : 465–544 nm; for red channel, λ_{ex} : 488 nm, λ_{em} : 592–679 nm; for TO-PRO-3, λ_{ex} : 633 nm, λ_{em} : 639–756 nm.

For dead/fixed cell staining, HeLa cells were seeded in a 35 mm glass-bottom tissue culture plate. After overnight culture, the cells were fixed with 70% ethanol, washed with PBS and stained with dye as per the previous protocol.

To create a live/dead cell pattern, HeLa cells were seeded in a 35 mm glass-bottom tissue culture plate. After attaching well on the bottom, the cells were fixed with 70% ethanol and washed three times with PBS. Live HeLa cells suspension was then seeded on the same dish. After overnight culture, the cells were stained using the same protocol as before.

Flow cytometry

HeLa cells were seeded and cultured overnight till ~80% confluency. Different stressors were then introduced. For dead cells, medium was removed and cells were re-suspended in 70% ethanol and kept for 10 minutes. For UV irradiation, cells were exposed to 200 Joules/meter² UV radiation and then cultured for another 24 hours. For heat-induced apoptosis, cells were kept in the incubator pre-heated to 55 °C for 2 hours, followed by normal culture for 12 hours. For chemotherapy drug, cells

were treated with 1 μ g/mL Nocodazole for 48 hours. After stress treatment, stressors were then removed and cells were washed for three times with PBS, followed by incubation with medium containing 4 μ M Silo-Cy or Silo-2Cy for 2 hours. Subsequently, cells were washed for three times with PBS and re-suspended in PBS for flow cytometric assay in three biological replicates. Signals were collected from green channel (λ_{ex} : 405 nm, λ_{em} : 510 \pm 50 nm) and red channel (λ_{ex} : 488 nm, λ_{em} : 670 \pm 14 nm) for Silo-Cy or Silo-2Cy by BD FACS Canto II. Flow cytometry data were analysed with FlowJo (Tree Star Inc.) and graphs were analysed in Prism 5.

Conflicts of interest

There are no conflicts to declare.

Acknowledgements

We thank Prof Patrick Humbert, Dr Ivan Poon, Prof Weisan Chen and Dr Kaye Truscott from La Trobe University for kindly providing the reagents, cell lines, software access and thoughtful discussion. We thank La Trobe Institute for Molecular Science Bioimaging Facility for the access of flow cytometers. This work was supported by grants to B.Z.T. [the University Grants Committee of Hong Kong (AoE/P-03/08), the Research Grants Council of Hong Kong (16305015, 16308016, C2014-15G, N-HKUST604/14 and AHKUST605/16), and the Innovation and Technology Commission (ITC-CNERC14SC01 and ITC PD/17-9)], J. L. (the Thousand Young Talents Plan of China and Hundred Talents Program of Zhejiang University) and Y.H. (Australian Research Council DE170100058 and Rebecca L. Cooper Medical Research Foundation PG2018043).

Notes and references

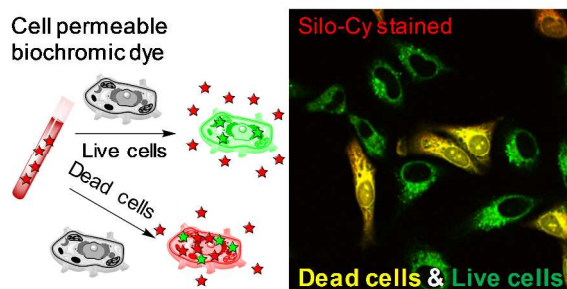
1. S. I. Han, et al., *BMB Rep*, 2008, **41**, 1–10.
2. C. W. Cotman and J. H. Su, *Brain Pathol*, 1996, **6**, 493–506.
3. K. Konstantinidis, et al., *Arterioscler Thromb Vasc Biol*, 2012, **32**, 1552–1562.
4. Y. Zheng, et al., *Arterioscler Thromb Vasc Biol*, 2011, **31**, 2781–2786.
5. B. Macchi, et al., *Mol Neurobiol*, 2014, **50**, 463–472.
6. A. Giordano, et al., *Curr Pharm Des*, 2012, **18**, 6331–6338.
7. M. Kato, et al., *Arthritis Rheumatol*, 2014, **66**, 40–48.
8. S. Y. Zhong, et al., *Br J Dermatol*, 2016, **174**, 542–552.
9. T. H. El-Metwally, *Cancer Biology: An Updated Global Overview*, Nova Science Publishers, 2009.
10. O. Kepp, et al., *Nat Rev Drug Discov*, 2011, **10**, 221–237.
11. T. L. Riss, et al., 2016.
12. X. Bai, et al., *J Biol Chem*, 2003, **278**, 35501–35507.
13. J. M. Brown and L. D. Attardi, *Nat Rev Cancer*, 2005, **5**, 231–237.
14. J. A. Rickard, et al., *Cell*, 2014, **157**, 1175–1188.
15. G. A. Cangelosi and J. S. Meschke, *Appl Environ Microbiol*, 2014, **80**, 5884–5891.
16. L. Galluzzi, et al., *Cell Death Differ*, 2018, **25**, 486–541.

17. G. Kroemer, et al., *Cell Death Differ*, 2009, **16**, 3-11.
18. M. J. Stoddart, *Mammalian cell viability: methods and protocols*, Humana Press, 2011.
19. I. Johnson and M. Spence, *Life Technologies Corporation*, 2010.
20. P. W. Sylvester, *Methods Mol Biol*, 2011, **716**, 157-168.
21. M. J. Stoddart, *Methods Mol Biol*, 2011, **740**, 1-6.
22. A. B. Lyons, et al., *Curr Protoc Cytom*, 2013, 9.11. 11-19.11. 12.
23. J. B. Grimm, et al., in *Fluorescence-Based Biosensors*, 2012, vol. 113, pp. 1-34.
24. J. Akagi, et al., *Cytometry A*, 2013, **83**, 227-234.
25. J. W. Lichtman and J.-A. Conchello, *Nat Methods*, 2005, **2**, 910-919.
26. S. Y. Ding, et al., *Sci China Chem* 2018, DOI: [s11426-018-9300-5](https://doi.org/10.1007/s11426-018-9300-5).
27. J. Mei, et al., *ACS Applied Mater Interfaces*, 2018, **10**, 12217-12261.
28. M. Gao and B. Z. Tang, *ACS Sens*, 2017, **2**, 1382-1399.
29. Y. F. Wang, et al., *Small*, 2016, **12**, 6451-6477.
30. S. Chen, et al., *Mater Horiz*, 2016, **3**, 283-293.
31. S. Chen, et al., *Chem Sci*, 2012, **3**, 1804-1809.
32. S. Chen, et al., *J Am Chem Soc*, 2013, **135**, 4926-4929.
33. H. Nie, et al., *Chem Eur J*, 2015, **21**, 8137-8147.
34. Y. Hong, et al., *Chem Soc Rev*, 2011, **40**, 5361-5388.
35. Y. Hong, et al., *Chem Commun*, 2009, 4332-4353.
36. J. Liu, et al., *Chem Rev*, 2009, **109**, 5799-5867.
37. Z. Zhao, et al., *Curr Org Chem*, 2010, **14**, 2109-2132.
38. H. B. Schmidt and D. Gorlich, *Trends Biochem Sci* 2016, **41**, 46-61.
39. C. C. Winterbourn, *Methods Enzymol*, 2013, **528**, 3-25.
40. S. Teramoto, et al., *Jpn J Pharmacol*, 1999, **79**, 33-40.
41. C. Castanier and D. Arnoult, *M S-Med Sci*, 2010, **26**, 830-835.
42. D. R. Green and F. Llambi, *Cold Spring Harbor perspectives in biology*, 2015, **7**.
43. S. Elmore, *Toxicol Pathol*, 2007, **35**, 495-516.
44. L. Jiang, et al., *Nat protocols*, 2016, **11**, 655-663.
45. M. G. Macey, *Flow Cytometry*, Springer, 2007.
46. A. Rehemtulla, et al., *J Biol Chem* 1997, **272**, 25783-25786.
47. Z. T. Gu, et al., *Sci Rep*, 2015, **5**.
48. R. J. Vasquez, et al., *Molecular biology of the cell*, 1997, **8**, 973-985.
49. T. H. Wang, et al., *J Biol Chem* 1998, **273**, 4928-4936.
50. N. Narayanan and G. Patonay, *J Org Chem*, 1995, **60**, 2391-2395.
51. P. J. Elving, et al., *Anal Chem*, 1956, **28**, 1179-1180.

Table of contents

Biochromic silole derivatives: a single dye for differentiation, quantitation and imaging of live/dead cells

Sijie Chen, Jianzhao Liu, Shouxiang Zhang, Engui Zhao, Yee Yung Yu, Roozbeh Hushiarian, Yuning Hong* and Ben Zhong Tang*



A new method using a single cell-permeable biochromic fluorescent dye to differentiate, quantitation and image both live and dead cells is reported.